

# A Search for PNe in Nearby Galaxies with SDSS Imaging Data

Alexei Y. Kniazev\*, Eva K. Grebel<sup>†</sup>, Daniel B. Zucker\*\*, Eric F. Bell\*\*, Hans-Walter Rix\*\*, David Martínez-Delgado<sup>‡</sup> and Hugh C. Harris<sup>§</sup>

\*European Southern Observatory, Karl-Schwarzschild-Strasse 2, 85748 Garching, Germany

<sup>†</sup>Astronomical Institute of the University of Basel, Venusstrasse 7, CH-4102 Binningen, Switzerland

\*\*Max-Planck-Institut für Astronomie, Königstuhl 17, D-69117 Heidelberg, Germany

<sup>‡</sup>Instituto de Astrofísica de Andalucía (CSIC), Camino Bajo de Hueter, 24 18008 Granada, Spain

<sup>§</sup>US Naval Observatory, Flagstaff Station, P.O. Box 1149, Flagstaff, AZ 86002-1149, USA

**Abstract.** We present the latest results from our project to search for new planetary nebulae in nearby galaxies using Sloan Digital Sky Survey (SDSS) imaging data. Our method is based on photometric criteria and can be applied to galaxies where PNe appear as point sources. We applied these criteria to the whole area of M31 as scanned by SDSS, detecting 130 new PN candidates and 30 known PNe. All selected PNe candidates are located in the outer regions of M31. For 85 candidates follow-up spectroscopy was obtained with the 2.2m telescope at Calar Alto Observatory. The observations show that our method has a detection efficiency of about 82%. We discuss the 2D velocity field of the outer part of M31 based on our observed PN data. The PNe suggest an exponential disk scale length of 13 kpc along the minor axis. We discovered two PNe along the line of sight to Andromeda NE, a very low surface brightness giant stellar structure in the outer halo of M31. These two PNe are located at projected distances of  $\sim 48$  kpc and  $\sim 41$  kpc from the center of M31 and are the most distant PNe in M31 found up to now. Our data support the idea that Andromeda NE is located at the distance of M31. No PNe associated with other M31 satellites observed by the SDSS were found. Applying our method to other SDSS regions we checked data for the Local Group galaxies Sextans, Draco, Leo I, Pegasus, Sextans B and Leo A and recovered a known PN in Leo A. We re-measured its O/H and for the first time determined abundances of N/H, S/H, He/H as well as the electron number density  $N_e$ . We argue that the PN progenitor was formed  $\approx 1.5$  Gyr ago during the strongest episode of star formation in Leo A.

**Keywords:** Spiral galaxies (M31), Dwarf galaxies, Physical properties (abundances, electron density), Planetary nebulae, Kinematics

**PACS:** 98.56.Ne, 98.56.Wm, 98.58.Ay, 98.58.Mj, 98.62.Dm

## INTRODUCTION

Planetary nebulae (PNe) arise from low-mass stars, making them excellent probes of the dynamics of low- to intermediate-mass stars in nearby galaxies. Their emission lines can provide accurate line-of-sight velocities within a minimum of telescope time. Therefore spectroscopy of PNe can be used as a powerful tool for the study of kinematics of nearby galaxies (e.g., Hurley-Keller et al. 2004), for the detection of new satellites (Morrison et al. 2003) and for the mapping of stellar accretion streams around large galaxies (Merrett et al. 2003). The spectra of individual PNe provide chemical abundances of certain elements, complementing photometric or spectroscopic metallicity information derived from old red giants, young supergiants, or H II regions. Searches for PNe are usually based on narrow-band imaging in the H $\alpha$  and [O III]  $\lambda$ 5007 lines, in which PNe can emit 15–20% of the luminosity of the central star.

The Sloan Digital Sky Survey (SDSS) (York et al. 2000) collects imaging data in drift-scan mode in five bandpasses ( $u$ ,  $g$ ,  $r$ ,  $i$ , and  $z$ ; Fukugita et al. 1996; Gunn et al. 1998; Hogg et al. 2001). These data are

then pipeline-processed to measure photometric and astrometric properties (Lupton et al. 2002; Stoughton et al. 2002; Smith et al. 2002; Pier et al. 2003). Since the detected flux from PNe comes almost entirely from nebular emission lines in the optical, the range of colors characteristic of the PNe is defined by the ratios of these emission lines and their corresponding contributions in different SDSS passbands. Some of these colors should be similar to the colors of emission-line galaxies (ELGs) and can be used for PN detection on the base of SDSS photometry.

## THE METHOD

We have developed a method to detect PN candidates in SDSS imaging data based on photometric criteria. Using an SDSS scan of M31 reduced with the standard pipeline (see Zucker et al 2004) and PNe from Nolthenius & Ford (1987) and Jacoby & Ford (1986) we constructed a test sample of previously known PNe with SDSS parameters. These were used to develop PN selection criteria based on their SDSS colors and magnitudes

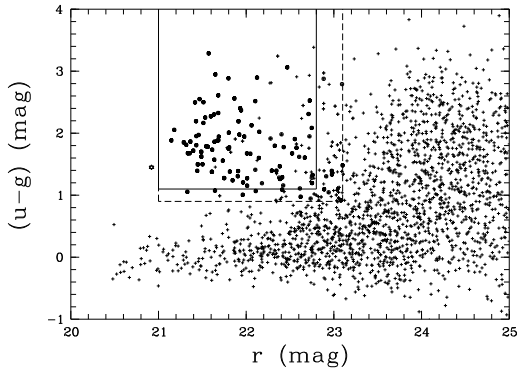


**FIGURE 1.** Color-magnitude diagram for stellar sources from the SDSS M31 data. All selected PN candidates of first priority are located within the region delineated by the solid lines. The dashed lines show the softer criteria for the selection of second priority candidates. All PNe from the test sample of previously known PNe as well as true PNe confirmed with spectroscopic follow-up observations are shown with filled circles. All PN candidates with follow-up observations that did not reveal obvious emission lines are marked by crossed circles. The one PN in Leo A is indicated by a star symbol.

(Kniazev et al. 2004a). We then applied these criteria to the whole area of M31 as scanned by the SDSS. The star–galaxy separation for the SDSS is better than 90% at  $r = 21.6^m$  (Abazajian et al. 2003), but worsens for fainter magnitudes. Thus we also applied the same selection criteria to extended objects. All candidates were visually verified to minimize false detections such as diffraction spikes of bright stars on SDSS images and clearly extended objects. Finally, we selected 105 PNe candidates that we labeled “first priority” (highly likely PNe) and 57 new PNe candidates labeled “second priority” (potential PNe; see Figure 1). All PNe from the test sample were detected as candidates of the first priority. With our final criteria we then applied our method to the whole SDSS data available on April 2004 and recovered a PN in the Local Group galaxy Leo A. No PNe were detected in other Local Group dwarfs covered by the SDSS: Sextans, Draco, Leo I, Pegasus and Sextans B. But for Leo I, Pegasus and Sextans B only photometry for the outer parts is available from the SDSS pipeline due to crowding.

We estimated possible contamination by point sources such as QSOs and stars, analyzing their distribution as given by Richards et al. (2002), and potential contamination by background emission-line galaxies, using data from Kniazev et al. (2004b). We find that our criteria select star-like sources far from both the QSO and stellar loci. There are only a few points located in our areas of interest, which would yield perhaps 1–10 objects per 1000 deg<sup>2</sup>. The numbers of ELGs in our sample should also be extremely small, since PNe stand out as being bluer in  $(g-r)$  vs.  $(r-i)$  and redder in  $(u-g)$  vs.  $(g-r)$

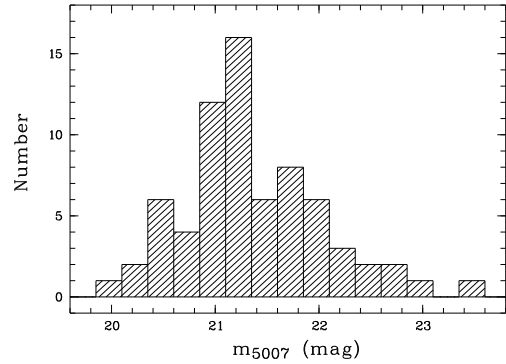


**FIGURE 2.** M31’s PN luminosity function from this work.

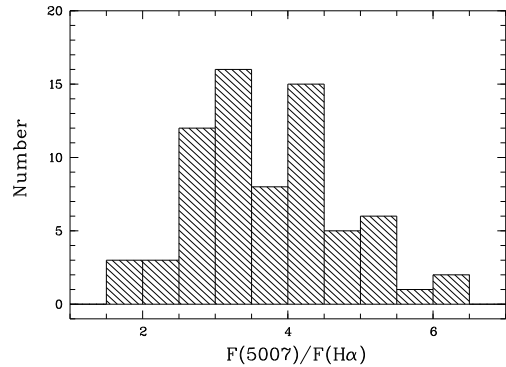


**FIGURE 3.** Observed [O III]  $\lambda 5007$  to  $H\alpha$  line ratio.

due to the contribution of the very strong emission lines  $H\beta$  and [O III]  $\lambda\lambda 4959, 5007$  in the SDSS  $g$ -band and  $H\alpha$  in the SDSS  $r$ -band.

## SPECTRAL FOLLOW-UP OBSERVATIONS

Spectroscopic follow-up observations of a subset of the detected M31 PNe candidates and of the PN in Leo A were carried out with the 2.2m telescope at Calar Alto Observatory in October and May 2004. We used the Calar Alto Faint Object Spectrograph (CAFOS). In 8 nights of observations under variable weather conditions a total of 85 PN candidates were observed. During these runs a long slit of variable width depending on the seeing and a G-100 grism were used. The effective wavelength coverage was  $\lambda 4200 - \lambda 6800 \text{ \AA}$  with dispersion  $\sim 1.9 - 2 \text{ \AA/pix}$  and a spectral resolution  $\sim 4 - 6 \text{ \AA}$  (FWHM). All data were reduced using MIDAS and IRAF and all emission lines were measured with the method described in detail in Kniazev et al. (2000) and Kniazev et al. (2004b).

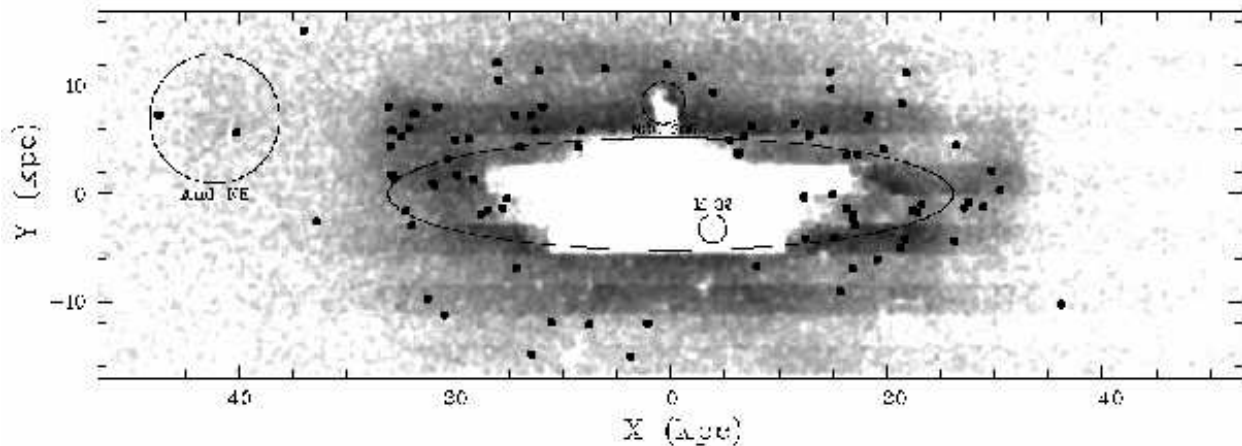


**FIGURE 4.** The spatial density of SDSS-detected stars is shown as a greyscale plot in the coordinates of the SDSS scans. The standard SDSS pipeline does not work properly in overcrowded fields, resulting in the lack of data in the central area of M31. The spatial distribution of newly-discovered PNe from the M31 SDSS data is overplotted by filled circles. The black ellipse indicates the approximate extent and inclination of the bright M31 disk. The large open circles mark the locations of NGC 205, M32 and And NE. The scale is plotted assuming a distance of 760 kpc to M31.

## RESULTS

### New PNe in M31

Out of the observed 85 PN candidates from the M31 SDSS data 70 turned out to be genuine PNe, which implies a total detection efficiency of 82%. Color-magnitude diagrams of the selected sources from SDSS M31 data and the results of our follow-up observations are shown in Figure 1. Figure 2 shows our PN luminosity function in terms of  $m_{5007}$  magnitudes calculated with the standard equation from Jacoby (1989). With our method we have found PNe over a range of 3 mag in the  $m_{5007}$ -band, the same magnitude range as in the earlier searches with narrow-band filters (Hurley-Keller et al. 2004).

The spatial distribution of the newly discovered PNe is shown in Figure 4. In part, they coincide with various well-known morphological features like *the Northern spur, the NE Shelf, the NGC 205 Loop, the G1 clump, etc.* which provides an opportunity to study abundances and velocities of these substructures of the outer part of M31. We discovered two PNe with projected locations near the center of And NE (Zucker et al 2004). This small number of PNe is consistent with the number to be expected in a stellar structure of this luminosity ( $\sim 5 \times 10^6 L_{\odot}$ ). With their projected distances of  $\sim 48$  kpc and  $\sim 41$  kpc from the center of M31 these are the most distant PNe possibly belonging to M31 found up to now.

The velocity distribution for all newly-discovered PNe along the major axis of M31 is shown in Figure 5. It is worth noting that most of them are rotationally supported

and trace the disk and/or bulge of M31, but do not show the signature of a kinematically hot halo where all objects would have random velocities. The calculated density profile of the new PNe shows an exponential decline with a scale length of  $\alpha = 12.6$  kpc along the minor axis of M31, which is very close to  $\alpha = 13.7$  kpc found by Irwin et al. (2005) using the Isaac Newton Telescope Wide Field Camera survey of M31.

The velocities of the two PNe in Andromeda NE are close to each other and agree well with the velocities of stars in this area (Ibata et al. 2005). They also fit in well with the continuation of the HI rotation curve from Kent (1989) (see Figure 5). Altogether with the results of our analysis of the spectroscopic line ratios our PN data support the idea that Andromeda NE is located at the distance of M31 and has  $[\text{Fe}/\text{H}] \approx -0.7$ .

### The PN in Leo A

Leo A is a nearby dIrr at a distance of 800 kpc (Dolphin et al. 2002) and a member of the Local Group. Strobel et al. (1991) detected an unresolved emission-line object as a PN candidate, which was then observed spectroscopically by Skillman et al. (1989), confirming its nature as a PN. These authors found an oxygen abundance of  $12+\log(\text{O}/\text{H}) = 7.30 \pm 0.16$  for this PN. This was the only spectroscopic measurement of the metallicity of Leo A to date. Our value of  $12+\log(\text{O}/\text{H}) = 7.38 \pm 0.14$  is in a good agreement with the earlier measurement. Translating this into  $[\text{Fe}/\text{H}]$  yields  $\approx -1.28 \pm 0.14$  ( $\sim 5.2\%$  solar), significantly more metal-rich than the photometrically derived metallicity

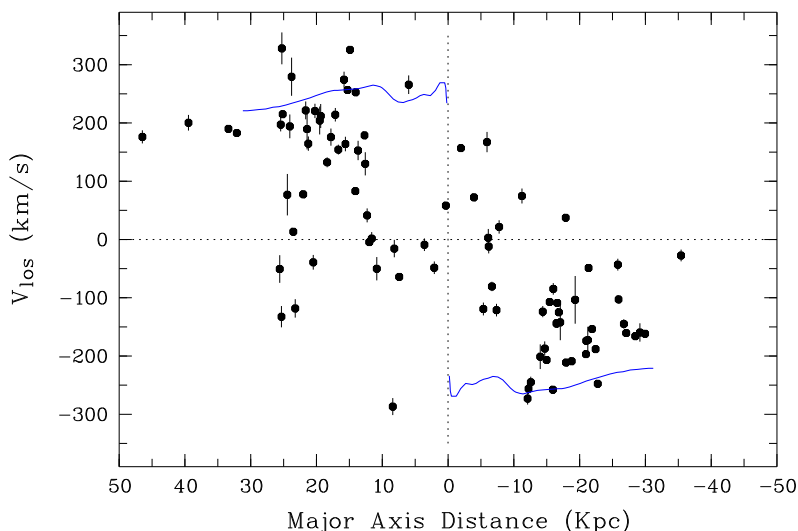


**FIGURE 5.** Velocity-distance diagram for newly discovered PNe in M31. The X-axis represents the projected distance along M31's major axis; the Y-axis shows the line-of-sight velocities. Filled black circles are new PNe from our survey. Errors of velocity determination are shown with bars. The line is the H I rotation curve from Kent (1989).

of Leo A's old population ( $-2.1$  dex, Grebel et al. 2003). We used our data to also measure for the first time the abundances of  $12+\log(\text{N}/\text{H}) = 6.70$ ,  $12+\log(\text{S}/\text{H}) = 4.60$  and  $12+\log(\text{He}/\text{H}) = 11.05$  as well as the electron number density  $N_e = 1800$  for this PN. Following the method described in Kniazev et al. (2005) we calculated a mass of ( $M/M_\odot \leq 1.5$ ) and an age of ( $t_{\text{MS}} < 1.6$  Gyr) for the progenitor of the PN. It would then have formed at the time when Leo A's star formation rate showed a marked increase (Tolstoy 1996).

## ACKNOWLEDGMENTS

The Sloan Digital Sky Survey (SDSS) is a joint project of The University of Chicago, Fermilab, the Institute for Advanced Study, the Japan Participation Group, The Johns Hopkins University, the Max-Planck-Institute for Astronomy (MPIA), the Max-Planck-Institute for Astrophysics (MPA), New Mexico State University, Princeton University, the United States Naval Observatory, and the University of Washington. Apache Point Observatory, site of the SDSS telescopes, is operated by the Astrophysical Research Consortium (ARC).

Funding for the project has been provided by the Alfred P. Sloan Foundation, the SDSS member institutions, the National Aeronautics and Space Administration, the National Science Foundation, the U.S. Department of Energy, the Japanese Monbukagakusho, and the Max Planck Society. The SDSS Web site is <http://www.sdss.org/>.

## REFERENCES

1. Abazajian et al. 2003, AJ, 126, 2081
2. Dolphin et al. 2002, AJ, 123, 3154
3. Fukugita, M., et al. 1996, AJ, 111, 1748
4. Grebel, E. K., et al. 2003, AJ, 125, 1926
5. Gunn, J.E., et al. 1998, AJ, 116, 3040
6. Hogg, D.W., et al. 2001, AJ, 122, 2129
7. Hurley-Keller, D., et al. 2004, AJ, 616, 804
8. Ibata, R., et al. 2005, AJ submitted (astro-ph/0504164)
9. Irwin, M., et al. 2005, ApJ in press (astro-ph/0505077)
10. Jacoby, G.H. 1989, ApJ, 339, 39
11. Jacoby & Ford 1986, ApJ, 304, 490
12. Kent, 1989, AJ, 97, 1614
13. Kniazev, A.Y., et al. 2000, A&A, 357, 101
14. Kniazev, A.Y. et al., 2004a, 19-21 May, ESO Workshop (Garching), "Planetary Nebulae beyond the Milky Way"
15. Kniazev, A.Y., et al. 2004b, ApJS, 153, 429
16. Kniazev, A.Y., et al. 2005, AJ, 130, 1558
17. Lupton, R.H., et al. 2002, Proc. SPIE, 4836, 350
18. Merrett et al., 2003, MNRAS, 346, L62
19. Morrison et al., 2003, ApJ, 596, L183
20. Nolthenius & Ford 1987, ApJ, 317, 62
21. Pier, J.R., et al. 2003, AJ, 125, 1559
22. Richards et al. 2002, AJ, 123, 2945
23. Skillman E.D., et al. 1989, ApJ, 347, 875
24. Strobel, N.V., et al. 1991, ApJ, 383, 148
25. Smith, J.A. et al. 2002, AJ, 123, 2121
26. Stoughton, C. et al. 2002, AJ, 123, 485
27. Tolstoy, E. 1996, ApJ, 462, 684
28. York, D.G. et al. 2000, AJ, 120, 1579
29. Zucker, D.B., et al. 2004, ApJ, 612, L117